

# Mechanosynthesis of perovskite $\text{LaGaO}_3$ and its effect on the sintering of ceramics

A. Moure<sup>a,\*</sup>, A. Castro<sup>b</sup>, J. Tartaj<sup>a</sup>, C. Moure<sup>a</sup>

<sup>a</sup> Instituto de Cerámica y Vidrio, CSIC, c/Kelsen, 5, 28049, Madrid, Spain

<sup>b</sup> Instituto de Ciencia de Materiales de Madrid, CSIC, c/Sor Juana Inés de la Cruz, 3 Cantoblanco, 28049, Madrid, Spain

Received 21 January 2009; received in revised form 5 February 2009; accepted 1 March 2009

Available online 27 March 2009

## Abstract

Ceramic precursors with  $\text{LaGaO}_3$  composition have been obtained by mechanosynthesis of a stoichiometric mixture of  $\text{La}_2\text{O}_3$  and  $\text{Ga}_2\text{O}_3$  after 34 h of milling. Single and crystalline phase powders can be obtained at a temperature as low as 800 °C; while by classical solid state reaction the  $\text{La}_4\text{Ga}_2\text{O}_9$  secondary phase still appears after calcination at 1200 °C. The influence of the mechanosynthesis route on the sintering of the ceramics has also been studied. The reduction of the particle size by prolonged milling and the higher reactivity of the activated precursors cause a reduction of the maximum shrinkage rate temperature of 500 °C with respect to the solid state reacted precursors. Despite these facts, it is found that the ceramics sintered from classically obtained precursors have similar densities at the optimum conditions as the ones obtained by mechanosynthesis, but with lower purity. Mechanical activation is shown as a good alternative to synthesize  $\text{LaGaO}_3$  based ceramics with Sr and Mg doping, which are candidates for electrolytes in solid oxide fuel cells (SOFC), but care with the sintering strategies must be taken into account to assure a high density of the ceramics.

© 2009 Elsevier Ltd and Techna Group S.r.l. All rights reserved.

**Keywords:** C. Ionic conductivity; E. Fuel cells; Mechanosynthesis

## 1. Introduction

Fuel cell is an electrochemical device that converts chemical energy into electrical energy and, on contrary to batteries, will work continuously consuming a fuel (generally hydrogen) of some sort [1]. They have received an increasing interest during the last years for the generation of energy because of its advantages with respect to the more widely used sources based on fossil combustible. They are energetically more efficient, because the generation of power is not limited by Carnot efficiency. Further their building is simplified because they do not contain any mobile parts. Environmental advantages must also be taken into account, as fuel cells can be considered as zero emission systems. When hydrogen is used as fuel, it only generates power and water.  $\text{CO}_2$  emission is eliminated. The basic concept of a fuel cell has three components: electrolyte,

anode and cathode. A first classification of fuel cells can be done regarding the nature of the electrolyte.

Within this classification, the fuel cells with a solid oxide as electrolyte (SOFC) are by now the ones with the largest theoretical efficiency, with values close to 60% in single cycle that can increase to 85% in cogeneration cycles of heat and electricity. Power densities in the order of 1–3 MW/m<sup>3</sup> are possible [2]. Zirconia based ceramics are the most common materials used as electrolyte. They have good mechanical properties and chemical stability, together with a high conductivity [1]. This is essential for SOFC applications. Values of ionic conductivity higher than 0.1 S/cm with low electronic conductivity ( $<10^{-4}$  S/cm) are found for the so-called yttrium stabilized zirconia (YSZ) compositions of  $\text{ZrO}_2$ , optimized by doping with 8% mol  $\text{Y}_2\text{O}_3$  [3]. These values are achieved at 900–1000 °C, which implies that high temperatures are needed for the cell to work. Efforts are focused now on reducing the operating temperature to 600–800 °C, with the advantages it presents: reduction of the material cost for the stacking of single cells, reduction of thermal isolation and increase of the cell mean life due to the decrease of thermal

\* Corresponding author. Tel.: +34 917355840; fax: +34 917355843.

E-mail address: [alberto.moure@icv.csic.es](mailto:alberto.moure@icv.csic.es) (A. Moure).

degradation and tension strains caused by the thermal cycles during operation [4]. Alternative materials are thus needed to reduce the operation temperature.

Ceramics with composition based on lanthanum gallate  $\text{LaGaO}_3$  have higher conductivity than YSZ materials when oxygen vacancies are created by doping with Sr and Mg [5–7], which make them good candidates for uses as electrolytes at intermediate temperatures (600–800 °C). The synthesis by classical methods of ceramics with Sr, Mg doped composition is difficult. Secondary phases [8], mainly  $\text{Sr}_3\text{La}_4\text{O}_9$ ,  $\text{SrLaGa}_3\text{O}_7$  and  $\text{SrLaGaO}_4$  are usually observed. They cannot be eliminated even at the highest sintering temperatures. These phases reduce the conductivity of the ceramics [9], besides the worsening of the mechanical properties [10]. Classical synthesis method by solid state reaction also involves high sintering temperatures that do not fully eliminate the secondary phases and that can lead to compositional inhomogeneities due to Ga evaporation [11].

Alternative processing methods are thus needed to resolve this issue. Mechanical activation has shown to be a successful route to improve the sinterability of the ceramic precursors, as part of the energy necessary to produce the chemical reaction is supplied by mechanical means. The reduction of the particle size and the high degree of homogeneity of the mixture of the starting materials (oxides, carbonates, hydroxides and others) during the prolonged milling [12] allows the reactivity of the precursors to be increased. The processing temperatures decrease, and phases that cannot be obtained by classical solid state reactions or that can be only stabilized by high-pressure techniques are achieved by mechanical activation [13]. The compaction density of the green pellet increases by particle size reduction [14]. It results in highly dense ceramics [15,16] in a single thermal process, and at lower temperatures than needed by classical means.

An understanding of the milling operation on the perovskite  $\text{LaGaO}_3$  doped with Sr and Mg is needed in order to apply this method to process electrolyte materials. With this aim, this work presents the results of the mechanosynthesis of  $\text{LaGaO}_3$  precursors using a mixture of  $\text{La}_2\text{O}_3$ – $\text{Ga}_2\text{O}_3$  for the first time to the author's best knowledge. Advantages over the classical solid state method have been established: reduction in the synthesis temperature of crystalline phase and in the sintering temperature. Ceramics prepared from both routes are studied for comparison. Differences in the sintering behavior between both routes and the effect in the final attained density are also discussed.

## 2. Experimental procedure

Mechanical activation was used to obtain the precursors of  $\text{LaGaO}_3$  ceramics, and the results were compared with the ones obtained by classical solid state reaction (SSR) method. For mechanically activated (MA) precursors, 3 g of a stoichiometric mixture of the  $\text{La}_2\text{O}_3$  and  $\text{Ga}_2\text{O}_3$  oxides were initially homogenized by hand mixing in an agate mortar and placed in a stainless-steel pot, with five 2 cm diameter, 35 g mass, stainless-steel balls. Mechanical activation was carried out

with a Pulverizette 6 model Fritsch planetary mill operating at 300 rpm. SSR precursors were obtained by thermal treatment at 1200 °C/4 h.

Phase compositions of the precursors and from sintered samples were analyzed by Bragg–Brentano X-ray diffraction (XRD) with a Bruker AXS D8 Advance diffractometer.  $\text{Cu K}\alpha$  radiation ( $\lambda = 1.5418 \text{ \AA}$ ) and a  $5 \times 10^{-2} \text{ }^\circ \text{ s}^{-1}$  scan rate were used. Both MA and SSR precursors were treated at several temperatures between 800 and 1500 °C, as detailed later, and characterized by XRD in a Siemens D5000 diffractometer, typically at  $3.3 \times 10^{-2} \text{ }^\circ \text{ s}^{-1}$  scan rate.

Initial oxide mixture and the one after prolonged milling were studied by Differential Thermal Analysis (DTA)–Thermogravimetric (TG) techniques. A thermoanalyzer Netzsch, model STA-409 was used up to 1200 °C, in an alumina crucible with a heating rate of  $5 \text{ }^\circ \text{C min}^{-1}$ .

X-ray fluorescence technique was used (spectrometer Phillips model PW-2424) to determine the possible contamination of the MA precursors. For the analysis, a sample of 0.3 g in fusion with 5.5 g of  $\text{Li}_2\text{B}_4\text{O}_7$  was prepared. Traces of  $\text{Fe}_2\text{O}_3$  were specially searched. It was estimated that the amount of iron oxide in weight% was  $1 \pm 0.2\%$ .

Quantities in the range of 0.7 and 1 g of the powders were uniaxially pressed in pellets with 0.8 mm diameter at  $1000 \text{ kg cm}^{-2}$  and then isostatically pressed at  $2000 \text{ kg cm}^{-2}$ . The shrinkage behavior was studied using a dilatometer Netzsch Gerätebau (model 402 EP, Selb-Bayern Germany) up to 1600 °C with heating and cooling rates of  $5 \text{ }^\circ \text{C min}^{-1}$ .

The SSR precursors were first attrition milled and sieved with a 100  $\mu\text{m}$  sieve to avoid the presence of large agglomerates. Green pellets were obtained by uniaxial pressing at  $1000 \text{ kg cm}^{-2}$ . Also, all the pellets were isostatically pressed at  $2000 \text{ kg cm}^{-2}$ . The samples were sintered in air at different conditions: 1400–1450 °C–12 h, 1500 °C–6 h for SSR precursors and 1200–1400 °C–12 h for mechanosynthesized powders, with different sintering strategies as explained below. All the heating rates were  $3 \text{ }^\circ \text{C min}^{-1}$ . Density of the ceramics was measured by Archimedes' method in distilled water at room temperature.

## 3. Results

Fig. 1 shows the evolution of the  $\text{La}_2\text{O}_3$  and  $\text{Ga}_2\text{O}_3$  mixture before and after milling at different times. At 1 h a broadening of the peaks due to the reduction of the particle size is observed. This situation is maintained up to 17 h, where peaks corresponding to the perovskite structure with  $\text{LaGaO}_3$  composition begin to appear. A mixture of phases is produced, as some peaks corresponding to the initial mixture are still observed, although their width and reduced relative height indicate a reduction in the size and crystallinity. At 34 h, the perovskite seems to be isolated as the only detectable phase. Traces of non-reacted initial oxides are not observed, although they can be present in small amounts or in amorphous form. Thus, it can be concluded that 34 h of milling is enough to mechanosynthesis single phase perovskite  $\text{LaGaO}_3$ , according to XRD.

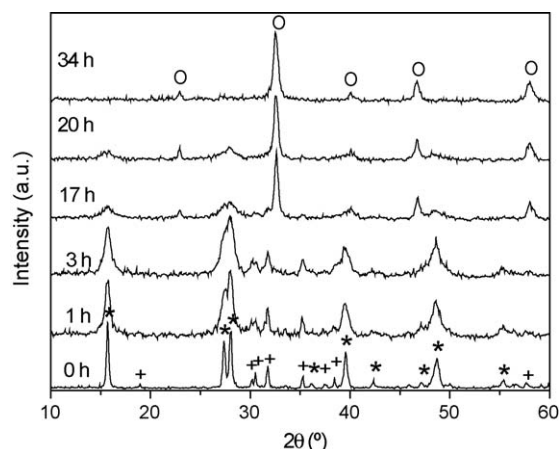


Fig. 1. XRD patterns of the stoichiometric mixture of  $\text{La}_2\text{O}_3$  and  $\text{Ga}_2\text{O}_3$ , precursor of  $\text{LaGaO}_3$  ceramics, before (0 h) and after different milling times [\* : initial  $\text{La}_2\text{O}_3$ ; + : initial  $\text{Ga}_2\text{O}_3$ ; O : mechano-synthesized  $\text{LaGaO}_3$ ].

Fig. 2 shows the DTA–TG evolution of the  $\text{La}_2\text{O}_3$  and  $\text{Ga}_2\text{O}_3$  mixture up to  $1200^\circ\text{C}$ . Weight loss is observed in three steps. The last two ones are related to two sharp endothermic peaks in the DTA curve. The region between  $500$  and  $1200^\circ\text{C}$  is amplified to better distinguish other two endothermic peaks near  $800^\circ\text{C}$  and between  $950$  and  $1050^\circ\text{C}$ .

Fig. 3 shows the DTA–TG evolution of the mechanochemically activated precursors, up to  $1500^\circ\text{C}$ . There are differences with the observations in Fig. 2. The three steps in the weight loss are now a continuous decrease with an inflexion at  $400^\circ\text{C}$  approximately, and an additional step at  $650^\circ\text{C}$  that does not appear for the oxide mixture. The related endothermic peaks are less sharp than the ones observed in Fig. 2. The total weight loss at  $1200^\circ\text{C}$  is lower for the mechanochemically activated than for the oxide mixture. The region between  $500$  and

$1200^\circ\text{C}$  is also amplified. The two endothermic peaks appearing at  $650$ – $700^\circ\text{C}$  seem to correspond to the ones appearing at  $950$ – $1050^\circ\text{C}$  in Fig. 2. At temperatures higher than  $1400^\circ\text{C}$  there are a number of peaks that can be attributed to structural phase transitions.

Fig. 4 shows the XRD pattern of the SSR precursor powder after calcination at  $1200^\circ\text{C}$ – $4$  h. A main perovskite phase is obtained, but with traces of  $\text{La}_4\text{Ga}_2\text{O}_9$  composition (JCPDF ICPD file no. 37-1433). This secondary phase appears typically in the synthesis of this composition by traditional SSR [17] in  $\text{LaGaO}_3$  powders. Fig. 5 shows the corresponding pattern after thermal treatment at  $800^\circ\text{C}$ – $4$  h of the mechano-synthesized precursor. Traces of secondary phases are not found. A reduction of more than  $400^\circ\text{C}$  is thus obtained with the use of MA to isolate  $\text{LaGaO}_3$  perovskite phase with higher purity than if SSR is used.

Figs. 6 and 7 show the dilatometric studies of  $\text{LaGaO}_3$  green pellets compacted from precursors obtained by SSR and mechano-synthesis, respectively. The curves of shrinkage and shrinkage rate are much simpler for the SSR precursors than for the mechano-synthesized ones. A contraction beginning at approximately  $1100^\circ\text{C}$  extends to  $1500^\circ\text{C}$ . The highest shrinkage rate is achieved at  $1450^\circ\text{C}$ , approximately. For the mechano-synthesized mixture, different shrinkage processes occur between room temperature and  $800^\circ\text{C}$ , approximately. Then there are two additional shrinkages, between  $850$  and  $1050^\circ\text{C}$  and between  $1100$  and  $1300^\circ\text{C}$ . A late contraction is observed between  $1350$  and  $1450^\circ\text{C}$ . This is the only one that is reversible, as it is observed as an expansion during the cooling of the sample (dashed line).

Pellets prepared from SSR precursors were sintered at  $1400^\circ\text{C}$ – $12$  h,  $1450^\circ\text{C}$ – $12$  h and  $1500^\circ\text{C}$ – $6$  h. The XRD patterns of the resulting ceramics are shown in Fig. 8. A

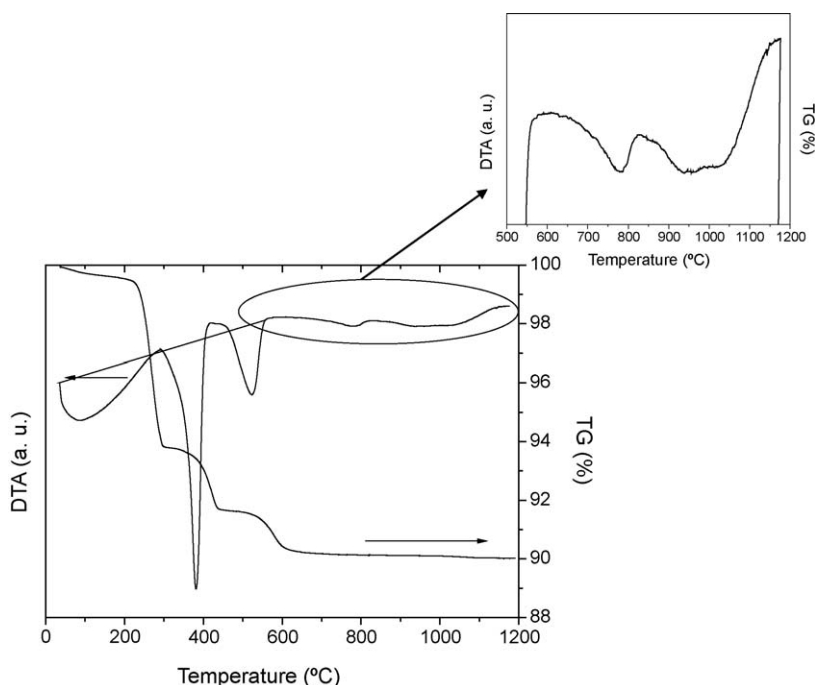


Fig. 2. DTA and TG curves of a mixture of  $\text{La}_2\text{O}_3$  and  $\text{Ga}_2\text{O}_3$ .

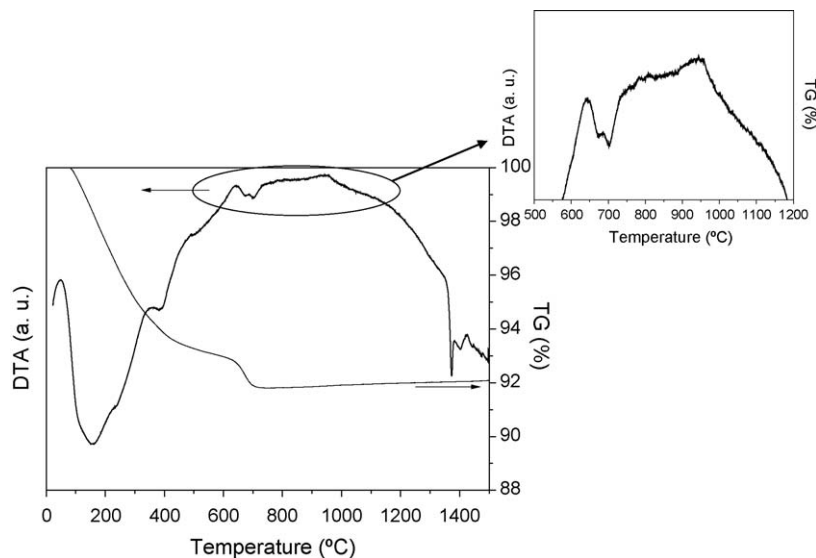


Fig. 3. DTA and TG curves of a mixture of  $\text{La}_2\text{O}_3$  and  $\text{Ga}_2\text{O}_3$  after 34 h of milling.

secondary phase begins to appear at increasing sintering temperatures, being clearly distinguished in the ceramic sintered at 1500 °C–6 h (marked with a circle). Fig. 9 shows the XRD patterns of the ceramics sintered from mechan-

osynthesized precursors. Single phase ceramics are obtained except for that sintered at 1400 °C–12 h. The secondary phases could not be identified with any structure containing La and/or Ga.

Table 1 shows the densification of the  $\text{LaGaO}_3$  ceramics measured by Archimedes' method. Values close to 95% are

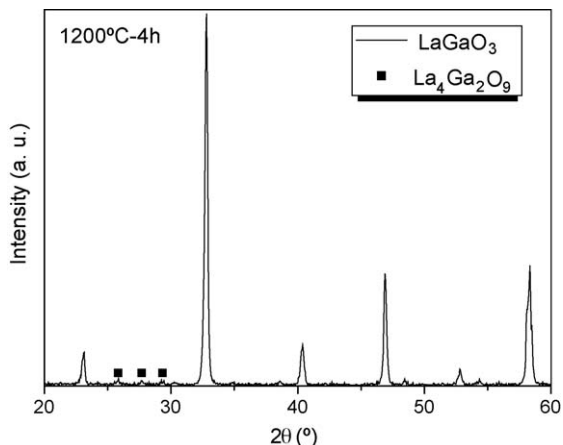


Fig. 4. XRD patterns after thermal treatment at 1200 °C–4 h of a mixture of  $\text{La}_2\text{O}_3$  and  $\text{Ga}_2\text{O}_3$ , precursor of  $\text{LaGaO}_3$  ceramics.

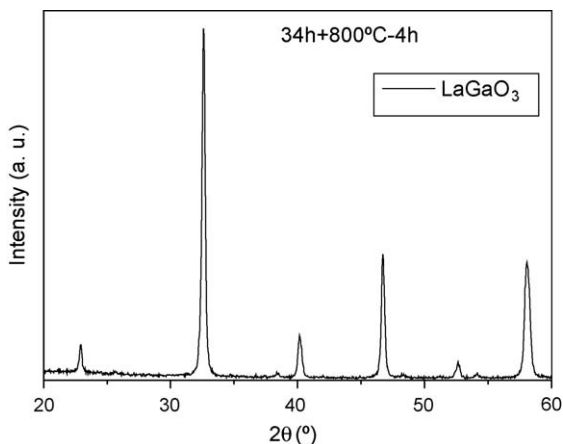


Fig. 5. XRD patterns after thermal treatment at 800 °C–4 h for the mechanosynthesized powder for 34 h of milling.

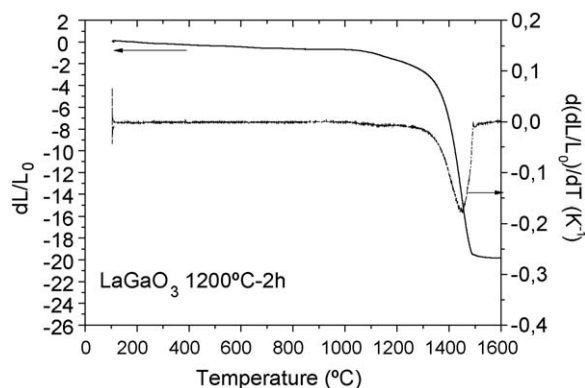


Fig. 6. Linear shrinkage and shrinkage rate of green pellets of  $\text{LaGaO}_3$ , from precursors obtained by solid state reaction.

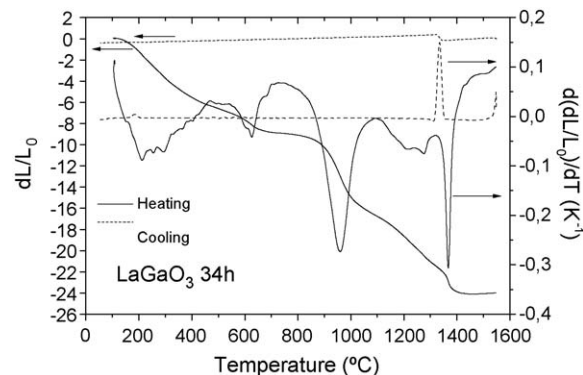


Fig. 7. Linear shrinkage and shrinkage rate of green pellets of  $\text{LaGaO}_3$ , from precursors obtained by mechanosynthesis after 34 h of milling. Dashed line: measurement on cooling.

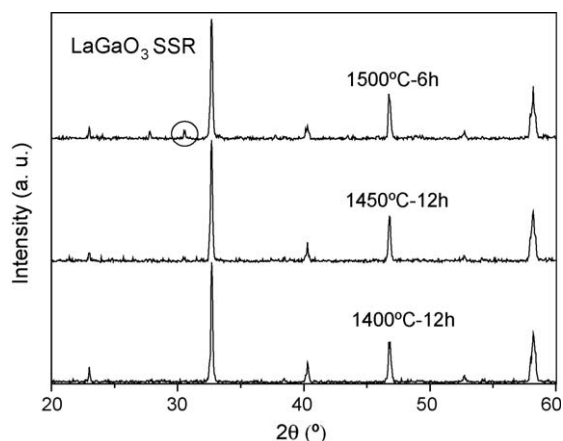


Fig. 8. XRD patterns of LaGaO<sub>3</sub> ceramics sintered from precursors obtained by solid state reaction.

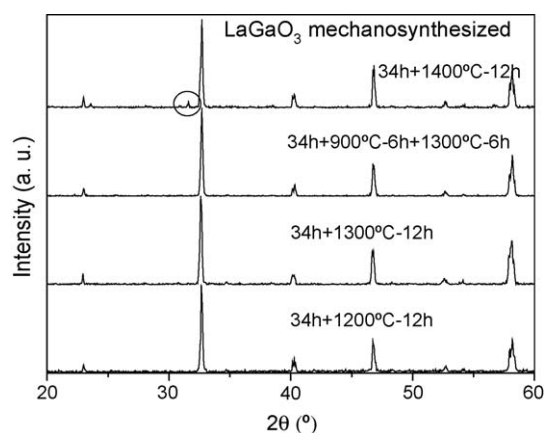


Fig. 9. XRD patterns of LaGaO<sub>3</sub> ceramics sintered from precursors obtained by mechanosynthesis after 34 h of milling.

found for the ones sintered from SSR precursors at 1400–1450 °C, and then they decrease when ceramics are sintered at 1500 °C-6 h. For the ceramics sintered at 1200–1400 °C from mechanosynthesized precursors, the sintering strategy was made by heating with two intermediate plateaus at 400 and 800 °C, based on the data of the shrinkage curve. Bubbles in the surfaces of the ceramic sintered at 1400 °C were observed. In addition, as Fig. 9 shows, secondary phases are found. No higher sintering temperatures were then checked. A new sintering heating curve was checked, with a plateau at the temperatures of the maximum shrinkage rate (900 °C-6 h) and final sintering at 1300 °C, also for 6 h (total sintering time of 12 h). Similar values of relative density are found to the ones obtained by single sintering at 1300 °C-12 h. In all cases, the

relative densities of the ceramics from mechanosynthesized precursors are in the same order than those found from SSR precursors. The maximum density for ceramics from mechanosynthesized precursors is achieved for sintering at 1300 °C (92%).

#### 4. Discussion

Differences in the behavior of the two LaGaO<sub>3</sub> precursors used are observed in the DTA–TG curves. The starting material for SSR is a mixture of oxides that transform to LaGaO<sub>3</sub> after heating. For the mechanosynthesized, the material is a perovskite powder obtained by milling, as observed by XRD.

The weight loss in three steps of the initial oxide mixture corresponds to the decomposition of La(OH)<sub>3</sub>, which is present at ambient atmosphere with La<sub>2</sub>O<sub>3</sub>. The sequence of the decomposition occurs in three stages [18]:

- (1) Elimination of absorbed water.
- (2) Dehydration of two molecules of water:  $2\text{La}(\text{OH})_3 \rightarrow 2\text{LaO}(\text{OH}) + 2\text{H}_2\text{O}$ .
- (3) Dehydration of one molecule of water:  $2\text{LaO}(\text{OH}) \rightarrow 2\text{La}_2\text{O}_3 + \text{H}_2\text{O}$ .

For the MA precursor, the weight loss can also be attributed to loss of water incorporated to the mechanosynthesized perovskite, but with different size and crystallinity that modify the way in which the water is incorporated to the material with respect to the non-milled La<sub>2</sub>O<sub>3</sub>. The additional step at 650 °C must be attributed to the loss of CO<sub>2</sub> from the carbonated state after milling [19]. The lower total weight loss for the mechanosynthesized mixture indicates that the perovskite can trap lower amounts of H<sub>2</sub>O.

The endothermic peaks at 800 °C and extended to 950–1050 °C for the oxides mixture, and at 650–700 °C for the mechanosynthesized one are due to the same phenomena, and are indicative of the differences between them. The peak at higher temperature is related to the formation of the perovskite through an intermediate La<sub>4</sub>Ga<sub>2</sub>O<sub>9</sub> phase (peak at lower temperatures) that still appears in XRD patterns shown in Fig. 4 after calcination at 1200 °C. The crystallization process is energetically more favorable in the mechanosynthesized product, as the endothermic peaks are closer one to the other than in the SSR precursor.

The crystallization of an isolated LaGaO<sub>3</sub> phase is achieved at lower temperatures (800 °C), as Fig. 5 shows, due to the high reactivity of the mechanosynthesized precursor. Comparing with SSR method, a reduction of more than 400 °C is achieved.

Table 1  
Densification of LaGaO<sub>3</sub> ceramics measured by Archimedes' method.

LaGaO <sub>3</sub> (solid state synthesis 1200 °C-2 h)				
Conditions		1400 °C-12 h	1450 °C-12 h	1500 °C-6 h
Density		94.8%Archimedes	95.4%	94.0%
LaGaO <sub>3</sub> (mechanosynthesis 34 h)				
Conditions	1200 °C-12 h	1300 °C-12 h	900 °C-6 h + 1300 °C-6 h	1400 °C-12 h
Density	84.8%	92.1%	92.6%	88.9%



Typical temperatures to obtain single phase in powder form are 1400 °C [20]. Different routes to the classical one for the synthesis of LaGaO<sub>3</sub> are barely found in the literature. Jena et al. reported pure phase at temperatures in the range of 720–820 °C [21] by metal nitrate–tartarate complex decomposition method. Kojima et al. recently used [22] a novel method of molten carbonates (with (Li<sub>0.435</sub>Na<sub>0.315</sub>K<sub>0.25</sub>)<sub>2</sub>CO<sub>3</sub>), reducing the synthesis to 500 °C, although the perovskite phase obtained was not completely pure. Moreover, mechanosynthesis route has the advantage of avoiding the necessary chemical steps in order to isolate pure enough phases.

The curves of shrinkage shown in Figs. 6 and 7 reveal differences between the sintering of both precursors. The contractions of the MA samples at temperatures lower than 800 °C are due to the loss of H<sub>2</sub>O and CO<sub>2</sub> trapped from the atmosphere in the mixture during milling, as it is produced in the same temperature range observed in the DTA/TG curves. It does not appear in the SSR precursors because the pressed material is totally composed by the perovskite and impurity phases, without trapped carbonates or water. The comparison of both curves shows that the sintering starts at a lower temperature (800, 350 °C lower) for the MA precursors than for the SSR ones, and with a higher velocity (maximum shrinkage rate of 0.29 K<sup>−1</sup> against 0.18 K<sup>−1</sup>). This is indicative of the higher reactivity achieved by mechanical activation. From the Scherrer equation [23] ( $t = 0.9\lambda/B \cos \theta_B$ , where  $\lambda$  is the wavelength used,  $B$  is the full width at half maximum of the diffraction peak and  $\theta_B$  is the Bragg angle), values of crystallite size in the order of 20 nm were calculated. Small particles allow a better compacting of the green pellet and the higher specific surface favors the closure of the porosity. Moreover, the prolonged milling introduces a number of defects that also favor the mass transport. A reduction of the sintering temperature to obtain similar or higher densification is expected. However, as observed in Table 1, the results are more complex.

The intermediate contractions in the mechanosynthesized precursors due to the elimination of gases, as water and CO<sub>2</sub> from the carbonated state after milling probably leads to the appearance of voids that are difficult to close at increasing temperature. It cannot be even ruled out that the secondary phases appearing in SSR precursors can play a role in sintering, pinning the grain boundaries and promoting the densification without grain growth and then achieving lower porosity. A strategy for emulating the same process with mechanosynthesized precursors with a long dwelling at 900 °C (maximum shrinkage rate) does not improve densification (Table 1). These results show the difficulty of the densification of LaGaO<sub>3</sub> ceramics at low temperatures, even with the use of alternative processing routes. As example, Jena et al. [21] reported values of density of 87% by sintering at 1350 °C from precursors obtained by metal nitrate–tartarate complex decomposition method. Results shown here are better even at lower sintering temperatures (1300 °C). It must be remarkable, however, that LaGaO<sub>3</sub> based ceramics for electrolyte applications are doped with Sr and Mg, that favor the densification of the ceramics [21]. Mechanosynthesis would provide a simplified method to process the ceramics in a unique thermal step, and with higher purity.

The appearance of the secondary phase after sintering at the highest checked temperatures (>1400 °C) seems to be related to the Ga loss. The variation of the ceramics weight before and after sintering from SSR precursors was slightly higher at 1500 °C (3.9%) than at 1400 and 1450 °C (3.6%). The amount of secondary phase is also higher, as Fig. 8 shows. Ga elimination gives place to Ga-deficient surfaces, favoring the formation of phases different than the perovskite one. Again, reduction of sintering temperature provided by mechanosynthesis would prevent this Ga elimination, achieving a higher purity of the ceramics.

## 5. Conclusions

Mechanosynthesis of LaGaO<sub>3</sub> perovskite phase has been obtained after 34 h of milling in a planetary mill of a La<sub>2</sub>O<sub>3</sub> and Ga<sub>2</sub>O<sub>3</sub> mixture for the first time. Pure and crystalline phases are obtained at 800 °C–4 h, reduction of more than 400 °C in temperature than when classical solid state reaction route is used.

Shrinkage studies show a complex sintering process in the mechanosynthesized precursors. Ceramics with similar porosity to the achieved with SSR precursors and with higher purity are obtained at lower sintering temperature.

Mechanosynthesis is a promising alternative for increasing the purity of LaGaO<sub>3</sub> based ceramics for SOFC applications, in which it is expected that the doping with Sr and Mg improves the densification of the ceramics. A simpler processing in a unique thermal step can be maintained, but control of the sintering strategies must be taken into account to assure a high densification of the ceramics.

## Acknowledgments

This work was supported by projects PROFIT CIT-120000-2007-50 and MICINN MAT2008-06785-C02-02-E. Dr A. Castro acknowledges the financial support of the Spanish MICINN (project MAT2007-61884). Dr. A. Moure is indebted to the CSIC (MICINN) of Spain for the “Junta de Ampliación de Estudios” contract (Ref JAEDOC087). The authors are grateful for the technical support provided by Ms I Martínez (ICMM).

## References

- [1] G. Hoogers (Ed.), Fuel Cell Technology Handbook, CRC Press, Boca Raton, FL, 2003.
- [2] S.P.S. Badwal, K. Foger, Solid oxide electrolyte fuel cell review, *Ceram. Int.* 22 (1996) 257–265.
- [3] E.C. Subbarao, H.S. Maiti, Solid electrolytes with oxygen ion conduction, *Solid State Ionics* 11 (1984) 317–338.
- [4] M. Dokiya, SOFC system and technology, *Solid State Ionics* 152 (2002) 383–392.
- [5] J.W. Fergus, Electrolytes for solid oxide fuel cells, *J. Power Sources* 162 (2006) 30–40.
- [6] P.N. Huang, A. Petric, Superior oxygen ion conductivity of lanthanum gallate doped with strontium and magnesium, *J. Electrochem. Soc.* 143 (1996) 1644–1648.
- [7] T. Ishihara, H. Matsuda, Y. Takita, Doped LaGaO<sub>3</sub> perovskite-type oxide as a new oxide ionic conductor, *J. Am. Chem. Soc.* 116 (1994) 3801–3803.

- [8] E. Djurado, M. Labeau, Second phases in doped lanthanum gallate perovskites, *J. Eur. Ceram. Soc.* 18 (1998) 1397–1404.
- [9] X.C. Lu, J.H. Zhu, Effect of Sr and Mg doping on the property and performance of the  $\text{La}_{1-x}\text{Sr}_x\text{Ga}_{1-y}\text{Mg}_y\text{O}_{3-\delta}$  electrolyte, *J. Electrochem. Soc.* 155 (2008) B494–B503.
- [10] M. Rozumek, R. Majewski, F. Aldinger, K. Kunstler, G. Tomandl, Preparation and electrical conductivity of common impurity phases in  $(\text{La},\text{Sr})(\text{Ga},\text{Mg})\text{O}_3$  solid electrolytes, *Cfi-Ceram. Forum Int.* 80 (2003) E35–E40.
- [11] W. Kunczewicz-Kupczyk, D. Kobertz, M. Miller, L. Singheiser, K. Hilpert, Vaporization of Sr- and Mg-doped lanthanum gallate and implications for solid oxide fuel cells, *J. Electrochem. Soc.* 148 (2001) E276–E281.
- [12] L.B. Kong, T.S. Zhang, J. Ma, F. Boey, Progress in synthesis of ferroelectric ceramic materials via high-energy mechanochemical technique, *Prog. Mater. Sci.* 53 (2008) 207–322.
- [13] M. Alguero, J. Ricote, T. Hungria, A. Castro, High-sensitivity piezoelectric, low-tolerance-factor perovskites by mechanosynthesis, *Chem. Mater.* 19 (2007) 4982–4990.
- [14] T. Hungria, M. Alguero, A. Castro, Synthesis of nanosized  $(1-x)\text{NaNbO}_3-x\text{SrTiO}_3$  solid solution by mechanochemical activation, processing of ceramics, and phase transitions, *Chem. Mater.* 18 (2006) 5370–5376.
- [15] S.E. Lee, J.M. Xue, D.M. Wan, J. Wang, Effects of mechanical activation on the sintering and dielectric properties of oxide-derived PZT, *Acta Mater.* 47 (1999) 2633–2639.
- [16] C.L. Chew, A. Srinivas, T. Sritharan, F.Y.C. Boey, Mechanochemical activation of strontium bismuth tantalate synthesis, *Scripta. Mater.* 53 (2005) 1197–1199.
- [17] M. Rozumek, P. Majewski, F. Aldinger, Metastable crystal structure of strontium- and magnesium-substituted  $\text{LaGaO}_3$ , *J. Am. Ceram. Soc.* 87 (2004) 656–661.
- [18] R.F.C. Marques, H.E. Zorel, M.S. Crespi, M. Jafellicci, C.O. Paiva-Santos, L.C. Varanda, R.H.M. Godoi, Thermal and crystallographic studies of mixture  $\text{La}_2\text{O}_3$ – $\text{SrO}$  prepared via reaction in the solid state, *J. Therm. Anal. Calorim.* 56 (1999) 143–149.
- [19] T. Hungria, A.B. Hungria, A. Castro, Mechanosynthesis and mechanical activation processes to the preparation of the  $\text{Sr}_2[\text{S}_{n-1}\text{Ti}_n\text{O}_{3(n+1)}]$  Ruddlesden–Popper family, *J. Solid State Chem.* 177 (2004) 1559–1566.
- [20] C.J. Howard, B.J. Kennedy, The orthorhombic and rhombohedral phases of  $\text{LaGaO}_3$ —a neutron powder diffraction study, *J. Phys. Condens. Matter.* 11 (1999) 3229–3236.
- [21] H. Jena, K.V.G. Kutty, T.R.N. Kutty, Novel wet chemical synthesis and ionic transport properties of  $\text{LaGaO}_3$  and selected doped compositions at elevated temperatures, *Mater. Sci. Eng. B: Solid* 113 (2004) 30–41.
- [22] T. Kojima, K. Nomura, Y. Miyazaki, K. Tanimoto, Synthesis of various  $\text{LaMO}_3$  perovskites in molten carbonates, *J. Am. Ceram. Soc.* 89 (2006) 3610–3616.
- [23] H.P. Klug, L.E. Alexander, *X-ray Diffraction Procedure of Polycrystalline and Amorphous Materials*, 2nd ed., John Wiley & Sons, New York, 1974.